Thermodynamic scaling Monte Carlo study of the liquid–gas transition in the square–well fluid

Nikolai V. Brilliantov and John P. Valleau

Citation: The Journal of Chemical Physics **108**, 1115 (1998); doi: 10.1063/1.475473
View online: http://dx.doi.org/10.1063/1.475473
View Table of Contents: http://scitation.aip.org/content/aip/journal/jcp/108/3?ver=pdfcov
Published by the AIP Publishing

Thermodynamic scaling Monte Carlo study of the liquid–gas transition in the square–well fluid

Nikolai V. Brilliantov[a] and John P. Valleau[b]
Chemical Physics Theory Group, Department of Chemistry, University of Toronto, Toronto, Ontario M5S 3H6, Canada

(Received 27 June 1997; accepted 10 October 1997)

A Temperature–and–Density–Scaling Monte Carlo (TDSMC) study of the square-well fluid was carried out. The relative excess free energy was obtained *directly* from the simulations with a standard deviation less then 0.5%. Energy, pressure, compressibility and heat capacity were calculated from the excess free energy data. For the system of 256 particles a reduced density interval of 0.1-0.68 and a reduced temperature interval of 1.053-1.29 was covered. In the simulations a ''zoom focus'' on the temperature–density grid was used: a ''panoramic view'' of the whole temperature–density region, on a relatively coarse grid, was combined with a ''close-up'' of the critical–point region, using a finer (T,ρ) grid. The coexistence curve was obtained with use of the double–tangent construction on the free energy, and the critical temperature and critical density were estimated. The critical parameters found by the TDSMC method are compared with those of other Monte-Carlo techniques. © *1998 American Institute of Physics.* [S0021-9606(98)52403-8]

I. INTRODUCTION

Several new Monte-Carlo (MC) techniques have been proposed recently to study the phase equilibria in two-phase systems.[1–8] It is not possible to simulate successfully two–phase states in MC experiments, although they would occur macroscopically, because the small systems used in simulations cannot support the free energy expense of creating a surface. In the Gibbs ensemble (GE) method the two phases are contained in separate periodic subvolumes, with particle and volume exchanges between the phases leading to equilibrium averages.[1–3] Alternatively, one may try to exploit the hypothesis of fluid-magnet universality (i.e. that the fluid and Ising criticality belong to the same universality class) and map the ''experimental'' density distribution of a critical fluid onto an Ising–model scaling function.[8] This mapping requires the fitting of some parameters by a procedure of uncertain reliability, even supposing that the universality hypothesis is correct. Finally, in the Temperature–and–Density–Scaling Monte Carlo (TDSMC) approach the coexistence curve is obtained by the *direct* calculation of the relative excess free energy as a function of temperature and volume[4–7] with subsequent application of the double tangent construction to find the densities of the coexisting phases at many temperatures. The advantage of this technique is that it provides direct simulation data, and it does not rely on the hypothesis of universality (for a discussion of the validity of the hypothesis of universality see e.g. Refs. 9, 10).

The TDSMC method has been applied successfully to study two-phase coexistence of the Lennard-Jones and Coulombic fluids.[7] In the present paper (paper I), which is the first of two directed to the further analysis of fluid phase–transition behavior, we report thermodynamic data for the square–well fluid, including the liquid–gas coexistence region, as studied by TDSMC. The coexistence curve obtained for the square-well fluid is also given here. In a second paper (paper II) we formulate an ''effective–Hamiltonian'' approach as a tool for studying the critical behavior of fluids and analyze within this framework our thermodynamic data and coexistence curve. We examine in this context conditions that should be fulfilled for the MC study of fluid criticality, and show that these conditions are indeed satisfied in our simulations.

The rest of the present paper (paper I) is organized as follows. In the next section we briefly sketch the basic ideas of the TDSMC method and discuss its advantages in application to phase coexistence studies. We also give some details about the practical application of this method. In Sec. III thermodynamic data from the TDSMC simulations are presented and discussed. In the last section, IV, we summarize our findings.

II. TEMPERATURE–DENSITY-SCALING MONTE CARLO FOR THE SQUARE–WELL FLUID

The method of Temperature–and–Density–Scaling Monte Carlo allows one to extract thermodynamic and structural properties of the model fluid throughout a wide range of densities and temperatures during a *single* Monte Carlo run. There are two main advantages of this method. One is that the relative free energies throughout the set of densities and temperatures are *directly* accessed from the MC data. Another is that the quasiergodicity problem, i.e. the possible trapping of the system in some subregions of configuration space, is avoided by virtue of the broad sampling distribution. These advantages are especially important in studying the critical behavior. Indeed, fluctuations, enhanced in the vicinity of the critical point, do not worsen noticeably the computational accuracy of the relative free energy. A detailed description of the TDSMC method may be found

[a]Also at Moscow State University, Physics Department, Moscow 119899, Russia; electronic mail: nbrillia@alchemy.chem.utoronto.ca
[b]Electronic mail: jvalleau@taurasi.chem.utoronto.ca

elsewhere.[4–7] Here we discuss the general idea of the method and explain some details of its practical application.

A. Temperature–density scaling Monte Carlo

In order to estimate the thermodynamic properties in some range $\rho^*_{\min} \leqslant \rho^* \leqslant \rho^*_{\max}$ of reduced density $\rho^* = \rho s^3$ and $T^*_{\min} \leqslant T^* \leqslant T^*_{\max}$ of reduced temperature $T^* = k_B T/\epsilon$ (where s and ϵ are, respectively, a characteristic length and energy of the interparticle interaction potential and k_B is Boltzmann's constant) one must generate an appropriate sampling distribution $\pi(\mathbf{r}^N)$, which will cover adequately the region of the configuration space $\mathbf{r}^N$ for N particles, important to all the states within the above ranges. If the configurations at different densities ρ_k are all to be represented in the *same* configuration space, it is necessary to use *reduced* coordinates

$$\mathbf{r} = \mathbf{q}/L_k, \tag{1}$$

where $\mathbf{q}$ is the position of the particle in real space and $L_k = V_k^{1/3}$, at the density $\rho_k = N/V_k$. Then the corresponding configuration integral $Z_{k,l}$ at (T_l, ρ_k) is given by

$$Z_{k,l} = V_k^N \int_{(1)} d\mathbf{r}^N e^{-\beta_l U(\mathbf{r}^N, L_k)} = V_k^N Z'(\beta_l, L_k), \tag{2}$$

which defines Z', where $\beta_l \equiv 1/k_B T_l$, and k_B is Boltzmann's constant, while $U(\mathbf{r}^N, L_k)$ is the energy at density $\rho_k = N/L_k^3$ corresponding to the reduced configuration $\mathbf{r}^N$. We can write $U(\mathbf{r}^N, L_k) = \Sigma_{i,j} \Phi(r_{ij}, s_k)$, where $\Phi(q_{ij}, s)$ is the interparticle interaction potential and $s_k = s/L_k$. It is easy to show[4] that, for any two states with (T_l, ρ_k) and $(T_{l'}, \rho_{k'})$,

$$\begin{aligned}
&\frac{\beta_{l'} A_{k',l'} - \beta_l A_{k,l}}{N} + \ln \frac{\rho_k}{\rho_{k'}} - \frac{3}{2} \ln \frac{T_l}{T_{l'}} \\
&\equiv \frac{\beta_{l'} A^{\mathrm{ex}}_{k',l'} - \beta_l A^{\mathrm{ex}}_{k,l}}{N} = \frac{1}{N} \ln \frac{Z'_{k,l}}{Z'_{k',l'}} \\
&= \frac{1}{N} \ln \left\{ \frac{\langle \exp[-\beta_l U(\mathbf{r}^N; L_k)]/\pi(\mathbf{r}^N) \rangle_\pi}{\langle \exp[-\beta_{l'} U(\mathbf{r}^N; L_{k'})]/\pi(\mathbf{r}^N) \rangle_\pi} \right\},
\end{aligned} \tag{3}$$

where $A_{k,l}$, $A^{\mathrm{ex}}_{k,l}$ are respectively the (Helmholtz) free energy and excess free energy of the state (T_l, ρ_k), and $\langle \cdots \rangle_\pi$ denotes an average on the distribution $\pi(\mathbf{r}^N)$.[4] Equation (3) shows that TDSMC allows one to calculate the *relative* excess free energy at each particular temperature and density (T_l, ρ_k), with respect to any reference point (T_0, ρ_0) ; $(k=0$ and $l=0$ are taken for the reference density and temperature). An *absolute* value of the excess free energy may be calculated if one also knows $A^{\mathrm{ex}}_{0,0} \equiv A^{\mathrm{ex}}(\rho_0, T_0)$. (The reference point may be taken at high temperature and low density, which may mean that one can estimate this value from a virial expansion for the free energy.[11])

It is straightforward, using Markov chain techniques,[12] to generate configurations $\mathbf{r}^N$ on a distribution proportional to any chosen $\pi(\mathbf{r}^N)$. The problem is in choosing an appropriate sampling distribution $\pi(\mathbf{r}^N)$: we adopt a procedure already tested[6,7] for the Lennard-Jones fluid. In this, we consider a weighted sum of Boltzmann distributions

$$\pi(\mathbf{r}^N) = \sum_l \sum_k W_{k,l} \exp[-\beta_l U(\mathbf{r}^N, L_k)] \tag{4}$$

over a grid of temperatures $T_l \equiv 1/k_B \beta_l$ and densities $\rho_k = N/L_k^3$ covering the ranges of interest. Choosing the weight factors $W_{k,l}$ as[6]

$$W_{k,l} \propto \exp(\beta_l A^{\mathrm{ex}}_{k,l}) \tag{5}$$

guarantees that each thermodynamic state of interest will be given equal weight in $\pi(\mathbf{r}^N)$; the grid of (β_l, ρ_k) must be sufficiently dense that there is a substantial overlap of the configurations from neighboring grid points.[6] It is easy, as in conventional MC work, to generate a Markov chain with the chosen limiting distribution $\pi(\mathbf{r}^N)$.

The quantities $A^{\mathrm{ex}}_{k,l}$ are not known in advance, however, and theoretical estimates may be used as a starting point. Fortunately, small systems are not very sensitive to the particular choice of $W_{k,l}$, so an adequate starting estimate for the relative excess free energy of a system with small N may easily be generated. The resulting TDSMC estimate for the excess free energy may then be used to calculate more precise values. Iterating this process a few times (two or three in practice) one obtains roughly coincident input and output values for the excess free energy; this signals a satisfactory sampling distribution and one can proceed to a ''production run.'' After obtaining precise results for the excess free energy for a system with a small number of particles N, one can use it to find a good starting estimate for the $W_{k,l}$, (5) of a larger systems of N' particles, by rescaling the $A^{\mathrm{ex}}_{k,l}$ with a factor N'/N. Then refinement as before will yield a good $\pi(\mathbf{r}^N)$ for the larger system.

One also needs to know an error estimate for the data; we address this question briefly. As usual in the MC simulations, the total Markov chain is divided into M consecutive blocks, and data for the separate block averages $\langle \exp[-\beta_l U(\mathbf{r}^N; L_k)]/\pi(\mathbf{r}^N) \rangle_\pi$ are collected. For the sake of convenience we denote these quantities $B_{k,l}$. The size of the blocks must be chosen sufficiently large (or grouped) to give essentially uncorrelated block averages of $B_{k,l}$ for successive blocks.[13] A straightforward (second-order) analysis of Eq. (3) shows that the variance of the quantity $(\beta_l A^{\mathrm{ex}}_{k,l} - \beta_0 A^{\mathrm{ex}}_{0,0})$ is given by the expression,

$$\sigma^2_{kl} + \sigma^2_{00} - 2\rho_{kl,00}, \tag{6}$$

where

$$\sigma^2_{kl} = \overline{(B_{kl} - \overline{B_{kl}})^2}/(M-1)\overline{B^2_{kl}}$$

is the variance of the block averages B_{kl}, and

$$\rho_{kl,00} = \overline{(B_{kl} - \overline{B_{kl}})(B_{00} - \overline{B_{00}})}/(M-1)\overline{B_{kl}}\,\overline{B_{00}}$$

is the covariance of B_{kl} and B_{00} (we use the obvious notation $\overline{X} = (1/M)\Sigma_i^M X_i$ for a quantity X, averaged over M blocks).

B. Application of the TDSMC to the square–well fluid

We perform the TDSMC study for a simple model interaction potential, the square–well potential, which is defined as follows:

$$\Phi(q_{ij};d,\lambda)=\begin{cases}+\infty & \text{if} \quad q_{ij}<d\\ -\epsilon & \text{if} \quad d\leqslant q_{ij}<\lambda d\\ 0 & \text{if} \quad q_{ij}\geqslant\lambda d,\end{cases} \tag{7}$$

where $q_{ij}\equiv|\mathbf{q}_i-\mathbf{q}_j|$ is the separation of particles i and j, and d is the hard-core diameter. In spite of its simplicity the square-well potential has the basic properties of a realistic potential (i.e. hard core plus attraction); it is widely used to model the interactions of uncharged colloidal particles (see e.g. Refs. 14, 15). Moreover, the square–well fluid may be considered as a convenient reference system in thermodynamic perturbation theory schemes,[11] and many approximate theories check their accuracy by application to the square–well fluid.[16] Here we report data for the relative excess free energy of this system obtained directly in the simulation, as well as other derived thermodynamic data, which may be applied to the properties of colloidal systems, or in order to check the accuracy of a scheme of theoretical approximations.

The reduced density and temperature of the square–well fluid are defined as $\rho^*=\rho d^3$ and $T^*=kT/\epsilon$, so that the interaction potential in the reduced–coordinate representation reads: $U(\mathbf{r}^N,L_k)=\Sigma_{i<j}\Phi(r_{ij};d_k,\lambda)$, where $d_k\equiv d/L_k$ and

$$\Phi(r_{ij};d_k,\lambda)=\begin{cases}+\infty & \text{if} \quad r_{ij}<d_k\\ -\epsilon & \text{if} \quad d_k\leqslant r_{ij}<\lambda d_k\\ 0 & \text{if} \quad r_{ij}\geqslant\lambda d_k.\end{cases} \tag{8}$$

We report a study of this fluid, with $\lambda=1.5$. Starting values for $A^{\mathrm{ex}}_{k,l}$ (cf. Eq. (5)) were taken from a fit to data obtained by Barker and Henderson.[11] After refining π by iteration as discussed above, the TDSMC estimate for the relative excess free energy was obtained for a small system ($N=27$). For a larger system, of 64 particles, a starting value of the relative excess free energy was obtained by then rescaling the results by a factor (64/27), and after a few iterations precise TDSMC data were generated. This procedure was repeated for systems of 125 and 256 particles. In the region of small densities ($\rho^*<0.15$) we found it useful to perform TDSMC simulations for systems with intermediate numbers of particles, namely of 45, 54 and 96 particles.

In order to calculate especially precise thermodynamic properties near the critical point, we combined two levels of detail in the calculations. Namely, we performed simulations for large ranges of temperature and density using a relatively coarse grid, and then focused on a small ''window,'' inside these ranges and surrounding the critical point, using a much finer grid. This provides more accurate data in the region around the critical point; the two sets of data were finally combined to give the free energy throughout the ranges, but with relatively high precision near the critical point.

Convergence of the MC runs for the square–well fluid turns out to be very much slower than for the comparable Lennard-Jones fluid;[6,7] this is presumably associated with the ''hard'' forces present in the model.

TABLE I. Technical data on the TDSMC runs: ρ^*–range indicates the reduced density range covered by the run, β^*–range the reduced inverse temperature range, while N is the number of particles, $n_{\rho,\mathrm{grid}}$ is the number of density grid points and $n_{T,\mathrm{grid}}$ is the number of temperature grid points. The last column indicates the number of MC steps.

N	ρ^*–range	$n_{\rho,\mathrm{grid}}$	β^*–range	$n_{T,\mathrm{grid}}$	No. Conf $\times10^{-7}$
256	0.10–0.16	77	0.75–0.95	8	14.0
	0.16–0.256	77		8	18.0
	0.256–0.4096	77		8	114.0
	0.4096–0.55	77		8	48.0
	0.55–0.68	77		8	14.0
	0.29–0.64	154	0.79–0.81	8	76.0
125	0.10–0.20	77	0.75–0.95	8	17.5
	0.20–0.40	77		8	17.5
	0.40–0.60	77		8	17.5
	0.60–0.80	77		8	17.5
	0.80–0.90	77		8	7.5
64	0.05–0.20	20	0.75–1.25	20	17.5
	0.20–0.40	20		20	8.0
	0.40–0.60	20		20	5.0
	0.60–0.80	20		20	5.0
	0.80–0.90	20		20	2.5
27	0.05–0.20	20	0.75–1.25	20	5.0
	0.20–0.40	20		20	1.0
	0.40–0.60	20		20	2.5
	0.60–0.80	20		20	2.5
	0.80–0.90	20		20	2.5

III. RESULTS AND DISCUSSION

A. Computational details

The TDSMC simulations were performed for square–well fluid systems of 27, 64, 125, and 256 particles. We used a linear grid for the inverse temperature and a grid linear in $\rho^{*2/3}$ for the reduced density. The overall density range was covered by five runs in adjoining density ranges.[17] All technical data including the number of temperature and density grid points, the number of MC configurations, and the density and temperature intervals used in the simulations, for all the systems studied, are given in Table I. For the system of 256 particles ranges of 0.1–0.68 for the reduced density ρ^* and 1.053–1.29 for the reduced temperature T^* were covered. In the following our discussion refers mostly to the 256-particle-system.

As usual the MC steps consisted of attempted trial moves of a single particle chosen at random; the new position was uniformly distributed in a small cubic box centered on the initial position and with a length giving a roughly 50% acceptance rate. The step $r\rightarrow s$ was of course accepted with probability $a_{rs}=\min(1,\pi_r/\pi_s)$, in an obvious notation, to give a limiting distribution proportional to π.

As usual in Thermodynamic–Scaling Monte Carlo,[4–6] the uniformity of the sampling over the density and temperature grid was monitored. For $N=256$ data was collected for eight temperatures and 381 densities, making 3048 thermodynamic states in all (see Table I), and for each state the reduced relative excess free energy (along with the potential energy) was calculated with respect to a reference state at $\rho_0^*=0.1$, $T_0^*=1.29$.[18]

In practice, for the five independent TDSMC runs performed for adjoining density intervals, the relative excess free energy was first calculated with respect to a reference state within the *particular* interval. In order to find the relative excess free energy of states within different runs, with respect to the *common* reference state ρ_0^*, T_0^*, one may match the relative excess free energy along the ''seams'' where the density intervals meet. For the five runs one has four density seams, where the densities of left and right density intervals coincide, and one needs to match the relative excess free energy of the left and the right intervals for the eight temperature grid points along each seam. This was done by choosing an additive constant for each run that shifts the *reference point* free energy of the right interval so that the values match as well as possible along the seam. Technically these constants were found by applying the least squares criterion. The variance of these additive constants were calculated using the variances and covariances of the values B_{kl} along the seam from the left and the right density intervals (i.e. of the values B_{kl} taken at the eight temperatures at the density of the ''seam''). The variance of the relative excess free energy of such thermodynamic states, with respect to a *common* reference state was then approximated by summing up the variances of these states with respect to their *particular* reference state, and the variances of the additive constants of any ''seams'' separating the two states; (a more exact treatment of the statistical error will be found elsewhere[7]).

Using the second and third virial coefficients for the square–well fluid, which are known exactly,[19] a quite accurate estimate for the *absolute* value of the excess free energy at low density may be obtained. In this way the absolute excess free energy of the reference point $\rho^*=0.1, T^*=1.29$ is estimated to be given by $\beta_0 A_{0,0}^{\mathrm{ex}}/N=-0.35192$. Thus one can estimate the *absolute* excess free energy of other states from the relation:

$$\frac{A^{\mathrm{ex}}(\rho_k,T_l)}{kT_lN}=\frac{\Delta A^{\mathrm{ex}}(\rho_k,T_l)}{kT_lN}-0.351\,92, \tag{9}$$

where $\Delta A^{\mathrm{ex}}(\rho_k,T_l)/kT_lN=(\beta_l A_{k,l}^{\mathrm{ex}}-\beta_0 A_{0,0}^{\mathrm{ex}})/N$ is obtained in the numerical simulations, using (3).

B. Thermodynamic data

In Fig. 1 this relative excess free energy is shown as a function of density for the different temperatures. The standard deviation of the relative excess free energy did not exceed 0.0035 for any of the thermodynamic states studied, and as is common for the TDSMC technique,[7] no drastic increase of this quantity near the critical point was observed.

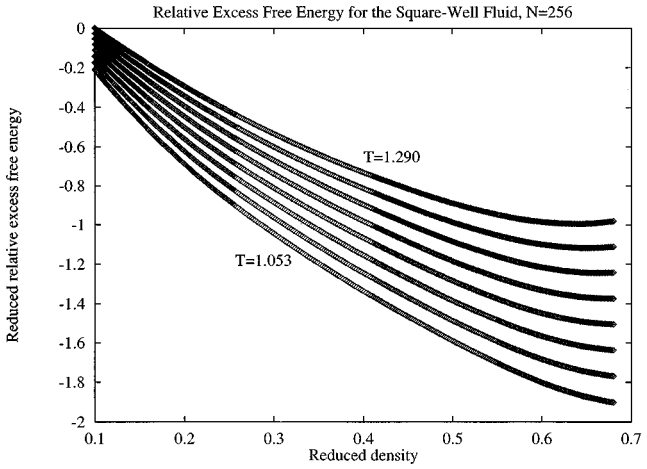

FIG. 1. Isotherms of the reduced relative excess free energy, $(A_{\mathrm{ex}}/Nk_BT)-(A_{\mathrm{ex}}/Nk_BT)_{\mathrm{ref}}$, for the square–well fluid. The reference state is $\rho_0^*=0.1$, $T_0^*=1.29$. The statistical errors are too small to show. The reduced temperatures from top to bottom are: 1.290, 1.250, 1.212, 1.176, 1.143, 1.111, 1.081, 1.053.

The availability of accurate TDSMC data in a wide density and temperature region enables one to extract the liquid–gas coexistence curve. The isotherms of total relative free energy, depicted in Fig. 2, show concave parts at the lower temperatures. This indicates the existence of a region unstable thermodynamically with respect to separation into two phases. The tangent points of the double tangent to these curves give estimates of the coexisting liquid and gas densities and its slope gives the vapor pressure. To simplify this analysis we made a global fit to represent all the relative free energy results. The excess free energy was expressed as a sum of the Carnahan-Starling term[11] appropriate to the hard-core interactions plus an additional expression (a Padé approximant) in which both the numerator and denominator were double polynomials in $\beta^{*\,1/2}$ and $\rho^{*\,1/2}$. These went to 5-th order in $\beta^{*\,1/2}$ and 6-th order in $\rho^{*\,1/2}$ (for details see Ref. 20). The deviation of the fit from the MC data did not

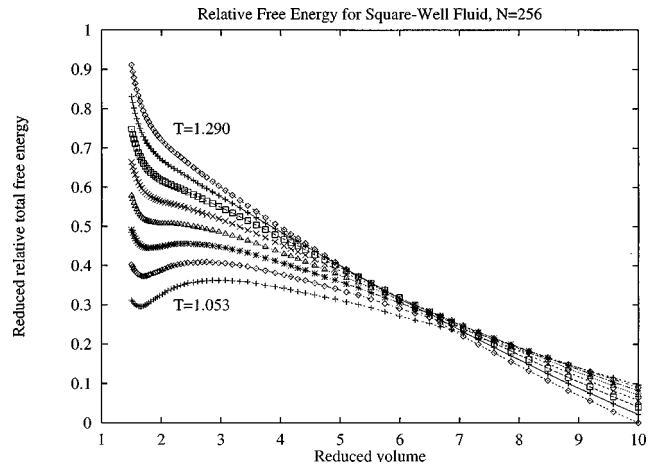

FIG. 2. Reduced relative total free energy, $(A/Nk_BT)-(A/Nk_BT)_{\mathrm{ref}}$. For clarity, data are plotted at only a subset of the 381 densities on each isotherm. The reduced temperatures from top to bottom are: 1.290, 1.250, 1.212, 1.176, 1.143, 1.111, 1.081, 1.053.

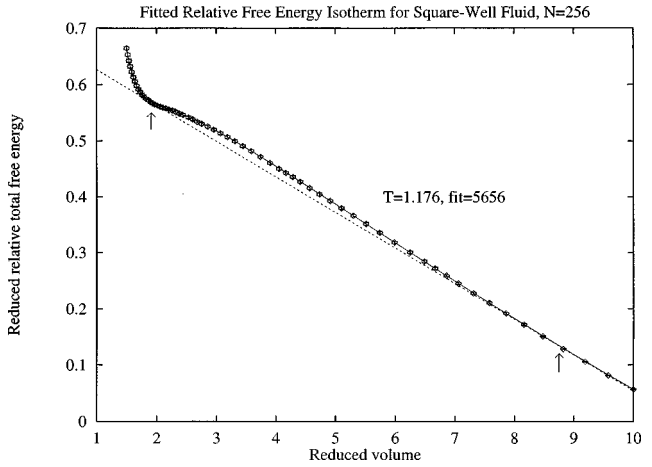

FIG. 3. Reduced relative total free energy, $(A/Nk_BT)-(A/Nk_BT)_{\mathrm{ref}}$, together with the 5656-analytical fit for one isotherm at $T^*=1.176$. Again only a part of the data are plotted. The arrows show the coexisting liquid and gas densities. The slope of the double tangent is $-P_{\mathrm{vap}}d^3/k_BT$.

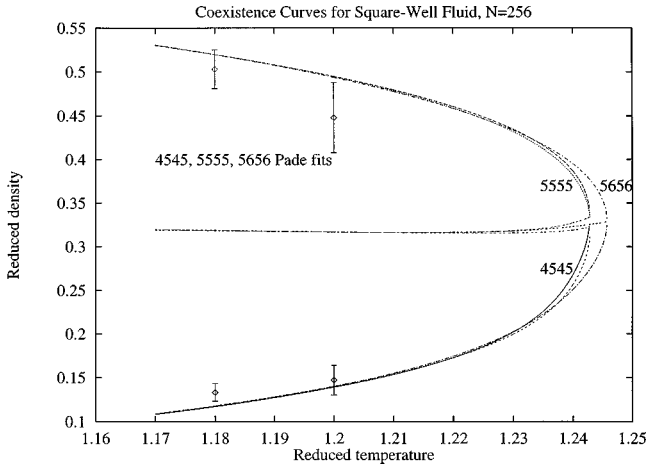

FIG. 4. Coexistence curves for the square–well fluid ($N=256$) obtained using different Padé approximants. The points are GEMC (Ref. 23) data. According to our estimates, the relative error for densities of the coexisting liquid and gas, $\delta\rho_{l,g}/\rho_{l,g}$, obtained from the TDSMC data, is definitely less then $(\delta A/\Delta A)P^*_{\mathrm{vap}}\kappa^*_{l,g}$, where δA is the error of the difference of relative excess free energies of the liquid and the gas, $\Delta A=A_l-A_g$, $\kappa^*_{l,g}=\kappa_{l,g}\epsilon/d^3$ is the liquid or gas compressibility on the coexistence curve for the finite–size system (which characterizes the curvature of the free energy curve at the coexistence points) and $P_{\mathrm{vap}}=P_{\mathrm{vap}}d^3/\epsilon$ is the reduced vapor pressure. For example, for $T^*=1.212$, we obtain $\delta\rho_l/\rho_l<0.006$, and $\delta\rho_g/\rho_g<0.057$.

exceed 0.05% for most of the thermodynamic states, where a fit with maximum flexibility was used (a ''maximum fit'' or 5656-fit). This is smaller than the apparent standard deviation for the free energy. The resultant analytic expression for the relative excess free energies was then used in the subsequent analysis of the thermodynamic data. In Fig. 3 TDSMC results along one isotherm of the relative free energy are compared with the results for the global fit, and the associated double tangent is also shown.

The fitted expression for the excess free energy was used to find the liquid and gas densities at various temperatures, by the double-tangent method, and thus the coexistence curve (and ultimately the critical point). We found that the coexistence curves, obtained using (analytical) fits with differing numbers of coefficients in the Padé approximant, say 4545, 5555 and 5656 gave nearly identical coexistence curves, but sometimes differed in the close vicinity of the critical point. To improve on this we performed, for $N=256$, an additional TDSMC simulation for a small ''window'' surrounding the estimated critical point, with a finer (T,ρ) grid. Explicitly, we studied the density interval $\rho^*=0.29-0.64$ and temperature interval $\beta^*=0.79-0.81$ with 154 density grid points and 8 temperature grid points. Finally, these ''close-up'' data for the excess free energy were combined with the previous ''panoramic'' ones and the Padé fits were

TABLE II. Gives the coefficients for the 5656-Padé fit for the $N=256$ system. These coefficients may be used to calculate the *relative* excess free energy, which is not affected by the arbitrary additive constant C used in our fitting procedure. For details of practical utilization of these coefficients see footnote 20.

			$T_{i,j}$		
$j\backslash i$	1	2	3	4	5
1	−5.256481	−4.931980	1.663360	0.244973	1.890508
2	8.330925	8.282495	5.792945	3.467952	2.219433
3	−3.673567	−15.769736	−12.061681	−12.163003	−11.995694
4	−4.810269	−20.064320	−6.996582	−2.703388	8.492503
5	7.569907	40.304974	21.145351	22.661093	26.656296
6	−3.136997	−11.702060	−12.598213	−17.226957	−31.181484
			$B_{i,j}$		
$j\backslash i$	1	2	3	4	5
1	0.636452	0.040154	−0.252615	−1.101554	−1.859788
2	0.468758	0.106463	0.006541	0.310797	1.501986
3	0.321868	0.471999	0.605576	2.527375	3.411022
4	0.310320	0.000296	−.141830	0.403983	0.905941
5	−3.787137	−3.757646	−4.005747	−6.404324	−6.214978
6	1.512073	3.848966	5.098054	5.290865	1.179715

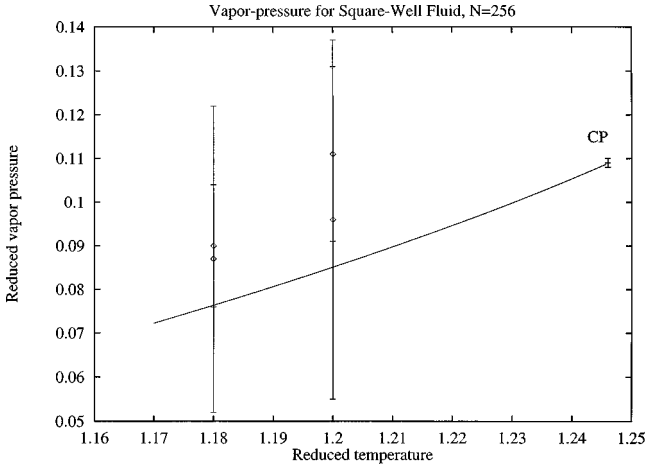

FIG. 5. Temperature dependence of the reduced vapor–pressure, $P^*_{\mathrm{vap}}=P_{\mathrm{vap}}d^3/\epsilon$ (where ϵ is the square–well depth), on the coexistence curve. The line shows present results; the points are the GEMC (Ref. 23) estimates for the pressure on the coexistence curve, estimated in the gas (upper points) and liquid. According to our estimates, the relative error for the vapor–pressure $\delta P_{\mathrm{vap}}/P_{\mathrm{vap}}$ obtained from the TDSMC, may be approximated by $\delta A/\Delta A$ (with the same notations as in the caption to Fig. 4). For example, for $T^*=1.212$, we estimate $\delta P_{\mathrm{vap}}/P_{\mathrm{vap}}\sim 0.011$.

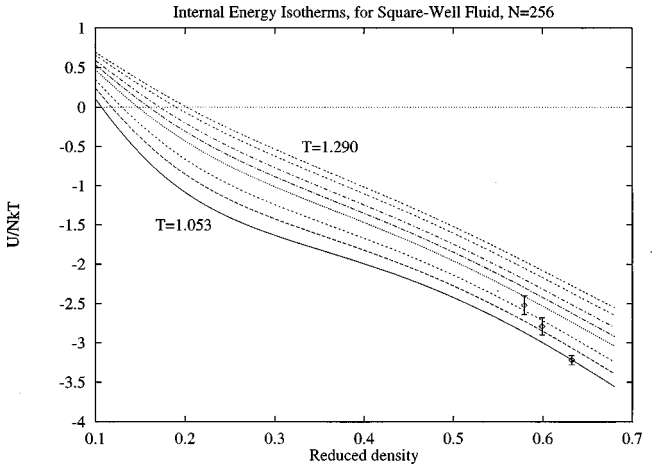

FIG. 6. Internal energy isotherms. The reduced temperatures from top to bottom are the same as on Fig. 2. The points are the GEMC (Ref. 23) data for the internal energy of the liquid phase at reduced temperatures 1.05, 1.08 and 1.10 close to ours. The errors for the internal energy are approximately of the same order as for the relative excess free energy.

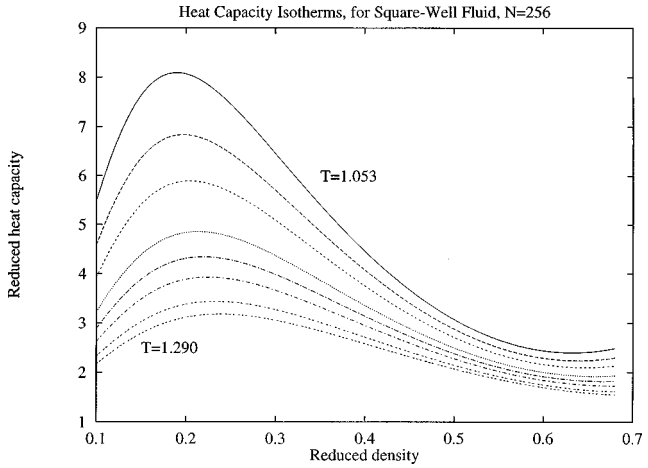

FIG. 8. Isotherms of the reduced heat capacity, C/Nk_B. The reduced temperatures from top to bottom are the same as on Fig. 2.

generated for the combined data (now a total of 4280 temperature and density points) (see Ref. 21). The Padé coefficients for the 5656-fit to these combined data, for $N=256$, are given in Table II; rather precise relative free energies may be calculated from these, using the functional form shown in Ref. 20 and Eq. (3).

Figure 4 shows that the resulting Padé fits obtained give pretty similar coexistence curves for the whole temperature and density range although the minimum 4545-fit has 40 coefficients, while the maximum 5656-fit has 60 coefficients. This encourages us to believe that the coexistence curves obtained in this way are reasonably accurate.

Figure 5 shows the temperature dependence of the vapor–pressure, corresponding to the 5656-fit coexistence curve, and Figs. 6–9 depict isotherms for the internal energy, pressure, heat capacity, and compressibility, obtained by analytical differentiation of the fitting function (5656-fit) for the relative excess free energy. One can clearly see the tendency to divergence of the heat capacity corresponding to critical behavior. For illustrative purposes we compare in Fig. 10 the coexistence curves for systems with different numbers of particles. For $N<256$ these curves were obtained without additional fine-grid simulations in the proximity of the critical point; we show curves resulting from the 5656-fits. As one can see from Fig. 10 the critical temperature gradually decreases with increasing size of the system, as expected, while the critical density practically does not depend on the size of the system.

Our results lead to estimates of the critical parameters for the small–N systems. For $N=256$ these are: $T_c^*=1.246\pm0.005$, $\rho_c^*=0.329\pm0.006$, and $P_c^*=P_c d^3/\epsilon=0.1090\pm0.001$. As discussed in the following paper (II),[22] the coexistence curves exhibit a finite–size crossover from roughly Ising–like behavior to roughly classical (mean–field) behavior as the temperature approaches the critical temperature from below. This means that the above finite–system critical temperature is higher than it would be if the Ising–like behavior persisted.

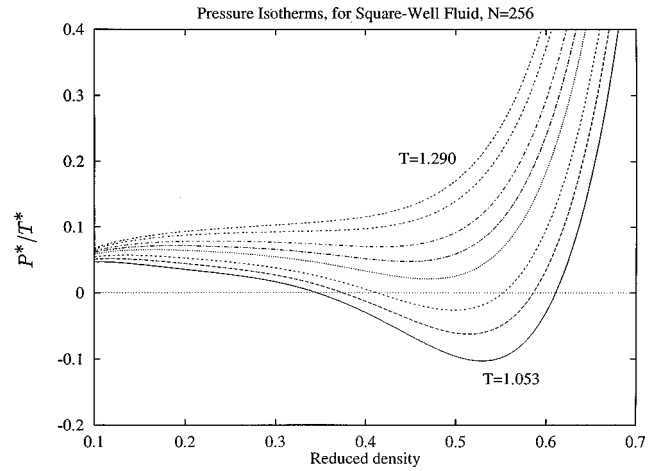

FIG. 7. Pressure isotherms. Reduced units for pressure, $P^*=Pd^3/\epsilon$, and for temperature, k_BT/ϵ, are used. The reduced temperatures from top to bottom are the same as in Fig. 2.

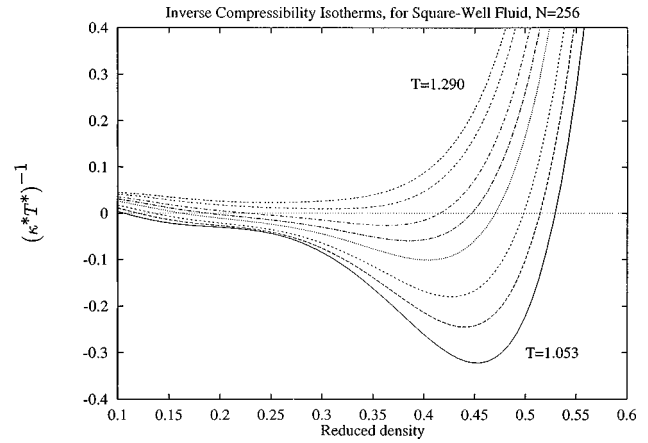

FIG. 9. Isotherms of inverse compressibility, $1/\kappa$. The inverse compressibility and temperature are given in the reduced units: $\kappa^*=\kappa\epsilon/d^3$, $T^*=k_BT/\epsilon$. The reduced temperatures are the same as on Fig. 2.

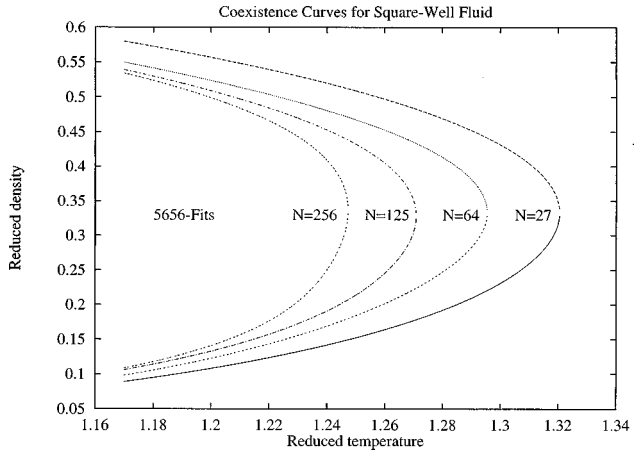

FIG. 10. Derived coexistence curves for the square–well fluid for 27, 64, 125 and 256 particles.

There have been some previous Monte Carlo estimates of these parameters. Of particular interest is the Gibbs–ensemble study of Vega, de Miguel, Rull, Jackson and McLure.[23] Rather large uncertainties in the coexisting densities are unavoidable, using this method, as the critical point is approached, and thus the data did not extend to temperatures very close to the critical point. To estimate the critical parameters the coexistence density data were extrapolated assuming an order-parameter exponent $\beta_{\rm fit}$ (with no Wegner correction terms) and a linear rectilinear diameter; the resulting best fitted value of $\beta_{\rm fit}=0.30\pm0.02$ (for $\lambda=1.5$) is roughly Ising–like. This extrapolation would ignore the finite–size crossover, so would be expected to lead to a critical temperature lower than that of the actual finite system. In fact the resulting estimate (for $N=512$ and thus an average of 256 particles in each phase, as in our case) was $T_c^*=1.219\pm0.008$, well below the above estimate. It turns out however to be below as well the value (roughly 1.24) corresponding to a similar extrapolation of our results (cf. paper II,[22] Fig. 5). The critical density was estimated at 0.299 ± 0.023, which is also lower than our results from thermodynamic scaling, although its large uncertainty makes the discrepancy marginal. Such discrepancies of Gibbs-ensemble results, with T_c and ρ_c both lower than should be expected for the (finite N) systems, have now been observed for several systems. They appear to be due to difficulties in implementing the Gibbs-ensemble simulations adequately as the critical region is approached, and this will be discussed elsewhere.[24] The reduced critical pressure of 0.108 ± 0.016 estimated using the Gibbs ensemble[23] agrees rather well with the present result, on the other hand (which is perhaps surprising in view of the temperature discrepancy).

Another set of critical parameters, $T_c^*=1.294$ and $\rho_c^*=0.317$ (for $N=154$) and $T_c^*=1.311$ and $\rho_c^*=0.327$ (for $N=110$) was obtained using an assumed form for an analytical extrapolation of fitted chemical potential data on a single slightly supercritical isotherm.[15] No error estimates were reported. The predicted critical temperature is much higher than our estimate; the N–dependence of critical temperature cannot explain such a discrepancy. Curiously enough, the critical density appears nevertheless to be rather close to ours.

More detailed analysis of the critical data is given in the subsequent paper II[22] and discussed in the light of an ''effective Hamiltonian'' approach.

IV. CONCLUSION

We have performed a Temperature–and–Density–Scaling Monte Carlo study of a square–well fluid. Data for the relative excess free energy, having standard deviations everywhere smaller than 0.5%, were obtained for systems of 27, 64, 125, and 256 particles. For the system of 256 particles the reduced density interval 0.1–0.68, and reduced temperature interval 1.053–1.29 were covered; a technique of performing supplementary study in the close vicinity of the critical point gave improved precision. From the estimated relative excess free energy in the temperature and density intervals studied we calculated the energy, pressure, heat capacity and compressibility as functions of temperature and density.

We found the liquid and gas coexistence densities from the relative free energies. The analysis was performed with the help of a double–Padé fit for the excess free energy of the $\sim$4000 states for which data was collected. From the liquid–gas coexistence curve, we obtained estimates of the critical temperature and the critical density which we believe to be more accurate than those given previously.

ACKNOWLEDGMENTS

We appreciate the financial support of the Natural Sciences and Engineering Research Council of Canada. Ian Graham very kindly provided the fitting program we used.

[1] A. Z. Panagiotopoulos, Mol. Phys. **61**, 813 (1987).
[2] A. Z. Panagiotopoulos, N. Quirke, M. Stapleton, and D. J. Tildesley, Mol. Phys. **63**, 527 (1988).
[3] B. Smit, Ph. de Smedt, and D. Frankel, Mol. Phys. **68**, 931 (1989).
[4] J. P. Valleau, J. Comput. Phys. **96**, 193 (1991); G. M. Torrie and J. P. Valleau, *ibid.* **23**, 187 (1977).
[5] J. P. Valleau, J. Chem. Phys. **95**, 584 (1991).
[6] J. P. Valleau, J. Chem. Phys. **99**, 4718 (1993).
[7] J. P. Valleau (in preparation); see also a review in Adv. Chem. Phys. (to be published); Ref. 6.
[8] N. B. Wilding and A. D. Bruce, J. Phys.: Condens. Matter **4**, 3087 (1992); A. D. Bruce and N. B. Wilding, Phys. Rev. Lett. **68**, 193 (1992); N. B. Wilding, Phys. Rev. E **52**, 602 (1995); J. Phys. Condens. Matter (in press).
[9] S.-K. Ma, *Modern Theory of Critical Phenomena* (Benjamin, New York, 1976)
[10] C. Vause and J. Sak, Phys. Rev. A **21**, 2099 (1980).
[11] J. A. Barker and D. Henderson, Rev. Mod. Phys. **48**, 587 (1976).
[12] J. P. Valleau and S. G. Whittington, *Statistical Mechanics, Part A: Equilibrium Techniques*, edited by B. J. Berne (Plenum, New York, 1977).
[13] In practice the Markov chains of $\sim10^7$–10^8 steps were divided into 50–100 blocks. With blocks of this size a further increase of the block size did not affect estimates of the standard deviations of the averages.
[14] P. Bolhuis and D. Frenkel, Phys. Rev. Lett. **72**, 2211 (1994).
[15] N. Ashiere, A. Lomakin, and G. B. Benedek, Phys. Rev. Lett. **77**, 4832 (1996); A. Lomakin, N. Asherie, and G. B. Benedek, J. Chem. Phys. **104**, 1646 (1996).
[16] D. Henderson, W. G. Madden, and D. D. Fitts, J. Chem. Phys. **64**, 5026 (1976); D. M. Heyes and P. J. Aston, *ibid.* **97**, 5738 (1992); F. D. Rio and L. Lira, Mol. Phys. **61**, 275 (1987); A. L. Benavides, J. Alejandre, and F. D. Rio, *ibid.* **74**, 321 (1991).

[17] In principle, one could cover the whole density range of interest in a single Monte Carlo run, but to speed the computations, the initial density interval can be divided into subintervals (Ref. 4). Indeed, due to the diffusive nature of MC sampling, the computation time necessary to cover some density interval grows eventually as the square of the interval length. Therefore, the time required to cover two large density intervals in two different runs is only two times larger then the time required for one interval, while performing a single run covering the doubled interval would require four times the computation time. However, it is not reasonable to use many *very* small density intervals, since every density ''seam,'' where these intervals must be matched together, introduces some extra errors into the resulting values of the relative excess free energies.

[18] Generally, one can use different grids in calculations of the sampling function and of the relative excess free energy (Ref. 4). In the present study we use the same grid for both calculations.

[19] J. O. Hirschfelder, C. F. Curtiss, and R. B. Bird, *Molecular Theory of Gases and Liquids* (Wiley, New York, 1954), p. 158.

[20] We used the following analytical fit for the excess free energy:

$$[A^{\mathrm{ex}}(\rho,T)/k_BTN]=[\eta(4-3\eta)]/(1-\eta)^2+\left[\sum_{i=1}^{5}\sum_{j=1}^{6}(\beta^*)^{i/2}(\rho^*)^{j/2}T_{i,j}\right]\times\left[1+\sum_{i=1}^{5}\sum_{j=1}^{6}(\beta^*)^{i/2}(\rho^*)^{j/2}B_{i,j}\right]^{-1}+C,$$

where $\eta=\rho^*\pi/6$, and C is an additive constant (estimated from the virial coefficients) which does not affect the values of the *relative* excess free energies. The coefficients $T_{i,j}$ and $B_{i,j}$ are given in Table II.

[21] In practice we found by least squares an additive constant that matched the TDSMC data of the small near-critical temperature–density window to the 5656-fit previously obtained for the rest of the data.

[22] N. V. Brilliantov and J. P. Valleau, J. Chem. Phys. **108**, 1123 (1998), following paper.

[23] L. Vega, E. de Miguel, L. F. Rull, G. Jackson, and I. A. McLure, J. Chem. Phys. **96**, 2296 (1992).

[24] J. P. Valleau, J. Chem. Phys. (to be published).